

Intermittent neural synchronization in Parkinson's disease

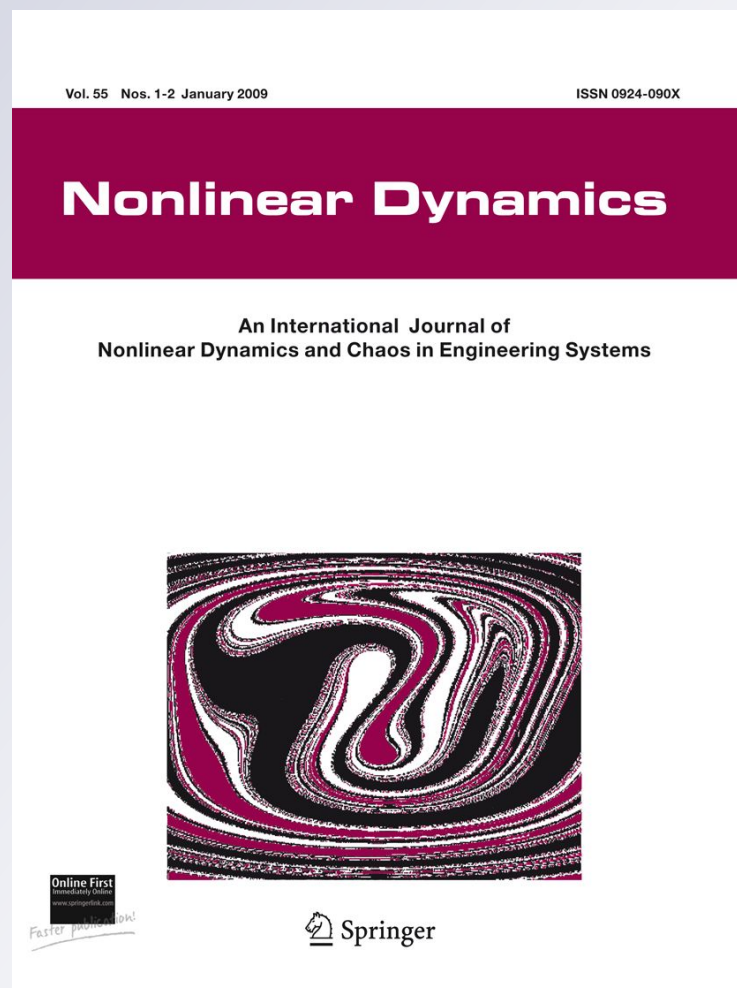
**Leonid L. Rubchinsky, Choongseok Park
& Robert M. Worth**

Nonlinear Dynamics

An International Journal of Nonlinear
Dynamics and Chaos in Engineering
Systems

ISSN 0924-090X
Volume 68
Number 3

Nonlinear Dyn (2012) 68:329-346
DOI 10.1007/s11071-011-0223-z



Your article is protected by copyright and all rights are held exclusively by Springer Science+Business Media B.V.. This e-offprint is for personal use only and shall not be self-archived in electronic repositories. If you wish to self-archive your work, please use the accepted author's version for posting to your own website or your institution's repository. You may further deposit the accepted author's version on a funder's repository at a funder's request, provided it is not made publicly available until 12 months after publication.

Intermittent neural synchronization in Parkinson's disease

Leonid L. Rubchinsky · Choongseok Park ·
Robert M. Worth

Received: 13 May 2011 / Accepted: 12 September 2011 / Published online: 8 October 2011
© Springer Science+Business Media B.V. 2011

Abstract Motor symptoms of Parkinson's disease are related to the excessive synchronized oscillatory activity in the beta frequency band (around 20 Hz) in the basal ganglia and other parts of the brain. This review explores the dynamics and potential mechanisms of these oscillations employing ideas and methods from nonlinear dynamics. We present extensive experimental documentation of the relevance of synchronized oscillations to motor behavior in Parkinson's disease, and we discuss the intermittent character of this synchronization. The reader is introduced to novel time-series analysis techniques aimed at the detection of the fine temporal structure of intermittent phase locking observed in the brains of Parkin-

sonian patients. Modeling studies of brain networks are reviewed, which may describe the observed intermittent synchrony, and we discuss what these studies reveal about brain dynamics in Parkinson's disease. The Parkinsonian brain appears to exist on the boundary between phase-locked and nonsynchronous dynamics. Such a situation may be beneficial in the healthy state, as it may allow for easy formation and dissociation of transient patterns of synchronous activity which are required for normal motor behavior. Dopaminergic degeneration in Parkinson's disease may shift the brain networks closer to this boundary, which would still permit some motor behavior while accounting for the associated motor deficits. Understanding the mechanisms of the intermittent synchrony in Parkinson's disease is also important for biomedical engineering since efficient control strategies for suppression of pathological synchrony through deep brain stimulation require knowledge of the dynamics of the processes subjected to control.

Keywords Intermittency · Phase locking · Phase synchronization · Basal ganglia · Subthalamic nucleus · Neuronal modeling

L.L. Rubchinsky (✉) · C. Park · R.M. Worth
Department of Mathematical Sciences and Center
for Mathematical Biosciences, Indiana University Purdue
University Indianapolis, Indianapolis, IN 46202, USA
e-mail: leo@math.iupui.edu

L.L. Rubchinsky
Stark Neurosciences Research Institute, Indiana University
School of Medicine, Indianapolis, IN 46202, USA

R.M. Worth
Department of Neurosurgery, Indiana University School
of Medicine, Indianapolis, IN 46202, USA

L.L. Rubchinsky
Department of Mathematical Sciences, Indiana University
Purdue University Indianapolis, 402 N. Blackford St.,
Indianapolis, IN 46202, USA

1 Introduction

Activity of neural circuits is a long-standing object of studies in nonlinear dynamics. Ideas, concepts and methods of nonlinear dynamics have been used to gain

insight into the function of neural systems (reviewed in, e.g., [1–4]). One of the important dynamical phenomena identified in these studies is synchronization. Different kinds of synchronization possible; however, what unites them is the temporal coordination of the dynamics [5].

Oscillations and synchronization in the brain are involved in a variety of brain functions, for example, perception, cognition, memory, and development [6–9], and also motor behavior [10–12]. Excessively strong, weak, or otherwise improperly organized patterns of synchronous oscillatory activity appear to contribute to the generation of symptoms of different neurological and psychiatric diseases [13–15]. The neuronal synchrony may be quite fragile and hard to detect. This may necessitate the use of time-sensitive data analysis methods, a trend which is noticeable in various areas of neuroscience [16]. Effective treatment strategies also call for better understanding of the mechanisms behind this kind of synchrony from a nonlinear dynamics perspective.

Parkinson's disease is one of the medical conditions where the symptoms are apparently related to pathologies of neural synchrony in certain brain regions. This review discusses this relationship and reviews recent results on synchronous Parkinsonian neurodynamics from both nonlinear time-series analysis and dynamical modeling perspectives. We also discuss the functional ramifications of recent experimental and modeling results and their potential importance for developing engineering methods to control brain synchrony in Parkinson's disease.

2 Basal ganglia motor circuits in Parkinson's disease

Parkinson's disease is a major neurodegenerative disorder characterized by chronic dopamine deficiency resulting in a set of primarily movement-related symptoms. The landmark of Parkinson's disease is overall slowness of movement. This hypokinetic behavior involves bradykinesia and akinesia (slowness of ongoing movement/inability to start new movement) and rigidity (stiffness of joints). Another important symptom is rest tremor, which occurs in a substantial number of Parkinson's disease cases, but probably has a different set of biological mechanisms and is not considered in this review.

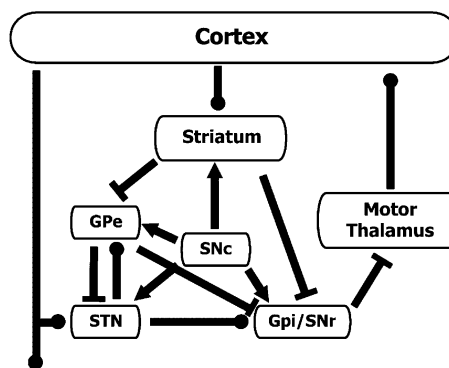


Fig. 1 Schematics of basal ganglia-thalamocortical circuitry. The basal ganglia receive inputs from cortical areas to striatum and subthalamic nucleus (STN), which is a major site for surgical interventions, and thus the main location from which intraoperative electrophysiological data are recorded. The output nucleus of the basal ganglia, Globus Pallidus pars interna (GPi), sends its projections to the thalamus as well as to the brainstem. Other depicted basal ganglia structures are Globus Pallidus pars externa (GPe), Substantia Nigra pars compacta (SNc), and pars reticulata (SNr), and striatum. Excitatory, inhibitory, and modulatory dopaminergic projections are presented in the diagram by circles, bars, and arrows, respectively. While the complete neuroarchitecture of these networks is more complicated, the diagram presents the major pathways

The loss of dopamine in Parkinson's disease is believed to directly affect a part of the brain called basal ganglia (see Fig. 1 for a schematic diagram of relevant neuroanatomy). The basal ganglia are a group of subcortical nuclei receiving extensive projections from cortex and sending extensive projections to the thalamus and which are, among other things, involved in the neural control of movement. The neurodegeneration in Parkinson's disease may extend beyond the dopaminergic system and the loss of dopamine may lead to a complex mix of direct and indirect consequences, slow compensatory response, etc. However, the changes in the dynamics of neural activity in the basal ganglia in Parkinson's disease (and in animal models of this disorder) are well documented in relation to the symptoms. For these reasons, the basal ganglia constitute the major surgical targets for ablative surgeries and deep brain stimulation (DBS) in Parkinson's disease.

One may, perhaps, identify two major questions in the science of Parkinson's disease. The first one is what triggers the neurodegeneration and what are the relevant molecular and cellular pathways, etc. The second is how and why the lack of dopaminergic modulation (and perhaps other neurodegenerative conse-

quences) translates into specific changes in the dynamics of neural activity, which in turn leads to the symptoms. In that sense, Parkinson's disease can be also viewed as a naturally occurring experiment, where parameters of the brain circuits are modified and the resulting dynamics can be observed. Thus, understanding of pathophysiology of the basal ganglia in Parkinson's disease may enhance the understanding of normal basal ganglia functioning.

Oscillations in the basal ganglia physiology, in particular in relation to motor control, are observed in different mammals (rodents, monkeys, humans), in different behavioral conditions and in different dopaminergic states (reviewed in [17–21]). Overall, the Parkinsonian low-dopamine state (Parkinson's disease in humans as well as pharmacologically induced dopaminergic lesions in rodents and nonhuman primates) is accompanied by an increase of oscillatory and synchronous activity [22–25]. Correlations of oscillatory activity between different locations in basal ganglia are variable, depend on the brain state, and are dynamically organized [26–28]. The spatial organization of synchronous patterns is also complex [27, 29–31].

The feedback circuits in basal ganglia [32, 33] and the rich membrane properties of basal ganglia neurons [34, 35] have been shown to support oscillations. In particular, oscillatory activity in the beta frequency band (loosely defined as activity around 20 Hz) is related to motor control and its alterations in the Parkinsonian state. Movement attenuates the power of and synchronization between basal ganglia activity and the cortical EEG [36] and attenuates synchronization between subthalamic nucleus (STN) neurons [37]. The strength of beta oscillations in STN local field potential (LFP) is inversely correlated with motor performance [38]. Single-unit STN recordings in PD yield similar results [39]. Note that LFP and single-unit recordings represent two different kinds of neuronal activity. The former is mostly formed by synaptic potentials, while the latter is mostly formed by the somatic and axonal electrical activity. However, both signals exhibit oscillatory dynamics in basal ganglia, apparently because somatic activity is influenced by synaptic activity and the oscillatory dynamics is exhibited by multiple basal ganglia—thalamocortical loops, rather than an oscillator confined to a single nucleus.

The action of dopaminergic medication on movement and synchronized oscillations fits this framework. Administration of L-DOPA (a major dopaminergic drug used in Parkinson's disease management)

decreases coherence between STN and GPi in the beta range [40], attenuates beta power in STN LFP [37, 41], and leads to similar effects in other parts of the basal ganglia-thalamocortical network [42]. The nonselective dopamine agonist apomorphine suppresses beta-band LFP activity in PD patients [43]; intraoperative injection of apomorphine in STN and pallidum leads to similar effects on spiking [37, 43]. Dopaminergic lesions in rodents increased LFP coherence across basal ganglia and cortex in beta-band. Application of apomorphine tends to partially reverse this effect [44]. Beta-band synchronization of the EEG from motor areas correlated with the severity of motor symptoms and decreased as the symptoms were alleviated by dopaminergic medication or DBS [45, 46].

One study observed correlations of beta-band activity in the maximally-symptomatic off-medication state with the degree of responsiveness to dopaminergic medication [47], which suggests that the action of dopaminergic agents may be more complicated than just suppressing the beta activity. However, overall dopamine-mediated changes in oscillatory activity are similar to the movement-induced changes. These findings seem to hold regardless of whether linear or nonlinear analysis is used [48] and are confirmed by more recent studies [49]. Therapeutic DBS, which improves motor symptoms, is also reported to decrease synchronized oscillatory activity in the beta-band [50–52].

All these studies have given rise to a “prokinetic gamma and antikinetic beta” paradigm [18–21, 53, 54] suggesting antikinetic character of beta-band activity. Beta-band activity has a normal physiological function [55], but its excess is pathological.

There are also a few experiments, which do not support a direct causal link between beta oscillations and slowness of movement. In the GPi of monkeys subjected to a progressive dopaminergic lesion, one group started to observe synchronized oscillatory activity *after* they detected motor impairment [56]. Similarly, there was an observation emergence of prominent beta oscillations *after* motor impairments in rodent models of Parkinson's disease [57]. However, the motor deficits seen in the aforementioned experiments could be of dystonic, not Parkinsonian nature [54, 57]. Furthermore, the difficulties of detection of variable weakly synchronized oscillations were acknowledged [56]. Thus, beta oscillations and motor activity are related when a change in the dopaminergic action is involved. The induction of beta-band oscillations in motor systems leads to slowness of movement not only in

Parkinsonian patients [58], but even in normal human subjects [59].

One need to keep in mind that Parkinsonian state may be much more than just the increased beta-band activity in STN. The Parkinsonian state may present not only changes in the oscillatory dynamics, but wider changes in the firing rates and patterns across multiple functional cortico-subcortical loops involving different parts of the basal ganglia, thalamus, and cortex [60, 61]. The involvement of cortical structures with basal ganglia oscillatory dynamics is natural given the anatomical and functional connections between cortex and basal ganglia. The complex structure of oscillatory cortico-basal ganglia correlations in different dopaminergic states has been studied in various contexts (e.g., [26, 27, 30, 31, 49]). Also, electrical stimulation in STN may exert its effect through the activation of specific cortical areas [62]. Even though many experimental studies in humans report the data recorded in STN (mostly because of STN happened to be a convenient and efficient neurosurgical target in Parkinson's disease), cortical areas as well as striato-pallidal circuits (which are investigated in animal studies, e.g., [28]) appear to be simultaneously involved in complex oscillatory dynamics.

Thus, we suppose the substantial relevance of beta-band oscillations to the motor deficits of a dopamine-deprived Parkinsonian state is supported by the large body of experimental evidence. Therefore, knowledge of the properties of these oscillations and their network and cellular mechanisms are of tremendous importance. These two issues are clearly connected. From the nonlinear dynamics perspective, the details of the temporal dynamics of these oscillations may help us to understand the properties of the underlying networks. The temporal dynamics of these oscillations on the short time-scales together with accompanying time-series analysis methods will be discussed in the next three sections. We then discuss how the resulting knowledge maybe used to gain insights into the dynamical mechanisms of the observed synchronous oscillations via modeling with coupled dynamical systems.

3 Variability of synchronized oscillations in Parkinsonian basal ganglia

One method for the management of advanced Parkinson's disease is functional stereotactic neurosurgery.

The neurosurgeon either makes a lesion in the basal ganglia or thalamus or implants an electrode in these structures, which is then connected to a high-frequency stimulator. In all cases, an essential stage of these procedures is microelectrode-guided targeting [63, 64]. A high impedance (of the order of 0.1–1.0 M Ω , as measured in the brain at 1 kHz or so) microelectrode is used for recording of neural activity in order to guide placement of the DBS electrode. The signal is usually high-pass filtered (300 Hz or above) to yield a time-series, suitable for the detection of extracellular spikes, and the same signal may also be low-pass filtered (200 Hz or below) to detect LFP. In case of the STN, synapses originate from projection fibers of neurons outside STN (we will discuss the origin of STN LFP in detail in Sect. 6). The extracellularly recorded high-frequency signal is used to discriminate spikes and subsequently to perform spike-sorting to obtain single unit activity.

Because of the importance of the beta-band oscillations, both time-series—continuous low-frequency LFP and binary (1 or 0) spiking signals—are band-pass filtered to the beta band. The result of the filtering of the spiking signal will no longer be “spiky”; it will be a continuous time-series, representing the modulation of the firing rate in the beta band. This appears to be appropriate for analyzing the original signal, as the bursts in the beta band represent pathological beta-band oscillations in the single unit signal, as we discussed above. A more detailed description of the sources, collection and pre-processing of the data can be found in [65]. An example of original and filtered time-series from the STN of a Parkinsonian patient is shown in Fig. 2. The spectra of these time-series are presented in Fig. 3; spectral peaks in the beta band are visible, but these peaks are relatively broad.

The patterns of synchronous oscillatory activity in basal ganglia are highly variable over short time intervals; this requires methods capable of detecting short episodes of synchrony. Thus, one needs to detect statistically significant episodes of synchronization. We will consider an approach developed in [66, 67].

First, signals are subjected to signal-to-noise ratio criteria to detect the episodes of oscillations in the beta band. Then an analysis of the phase locking is performed. The phase of the neuronal signals is presumed to be important and phase synchronization is a generic phenomenon in networks of oscillatory elements [5]. A traditional and robust way to recover the phase of

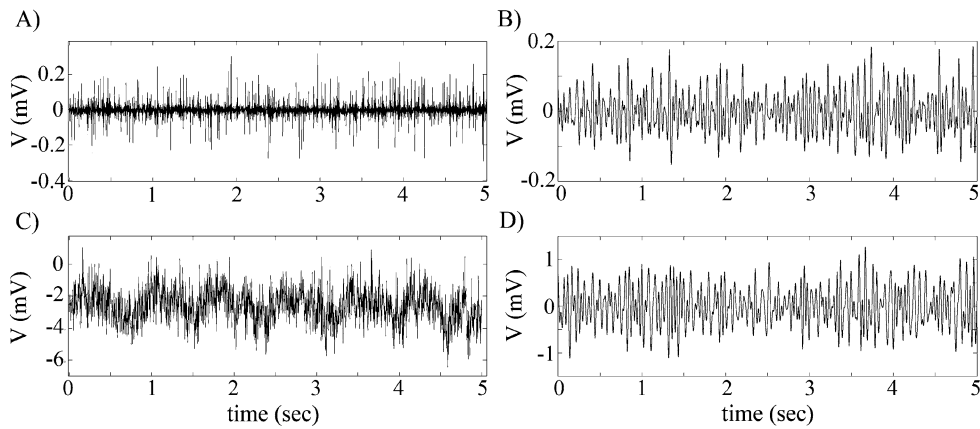


Fig. 2 Electrical activity of Parkinsonian basal ganglia. **A** is raw recordings of extracellular unit (spiking signal); **C** is recordings of LFP signal. The signals are modulated in many different ways. Because of the relationship between beta-band activity and Parkinsonian motor symptoms, the episodes with signifi-

cant oscillatory activity in the beta band were detected and the data from these episodes are band-pass filtered to the beta band only, resulting in a more sine-like spiking signal (**B**) and LFP signal (**D**)

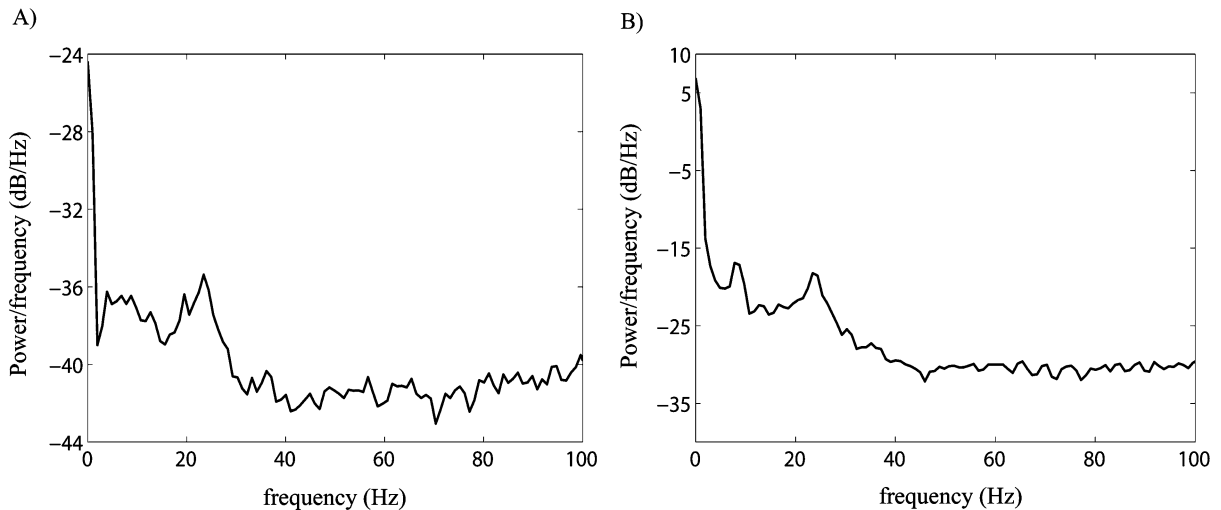


Fig. 3 Fourier spectra of extracellular spiking unit (**A**) and LFP (**B**) recorded in STN of a Parkinsonian patient. In both cases, there is a relatively broad peak in the beta frequency band

an oscillatory signal is to use the Hilbert transform to obtain an analytic signal $\zeta(t)$ from the real time-series $x(t)$; $\varphi(t)$ (the phase of the complex variable $\zeta(t)$) is the Hilbert phase of the time series. Alternative phase reconstruction methods give similar results [68]. The continuous analog of the operation is:

$$\zeta(t) = x(t) + i\bar{x}(t)$$

$$\bar{x}(t) = H(x) = \frac{1}{\pi} P.V. \int_{-\infty}^{\infty} \frac{x(\tau)}{t - \tau} d\tau$$

$$z(t) = \frac{\zeta(t)}{\|\zeta(t)\|} = e^{i\phi(t)}$$

Phases $\varphi_{\text{spikes}}(t)$, $\varphi_{\text{LFP}}(t)$ and phase difference $\Phi_j = \varphi_{\text{spikes}}(t_j) - \varphi_{\text{LFP}}(t_j)$ for spikes and LFP are constructed and we consider

$$\gamma_N(t_k) = \left\| \frac{1}{N} \sum_{j=k-N}^k e^{i\Phi_j} \right\|^2$$

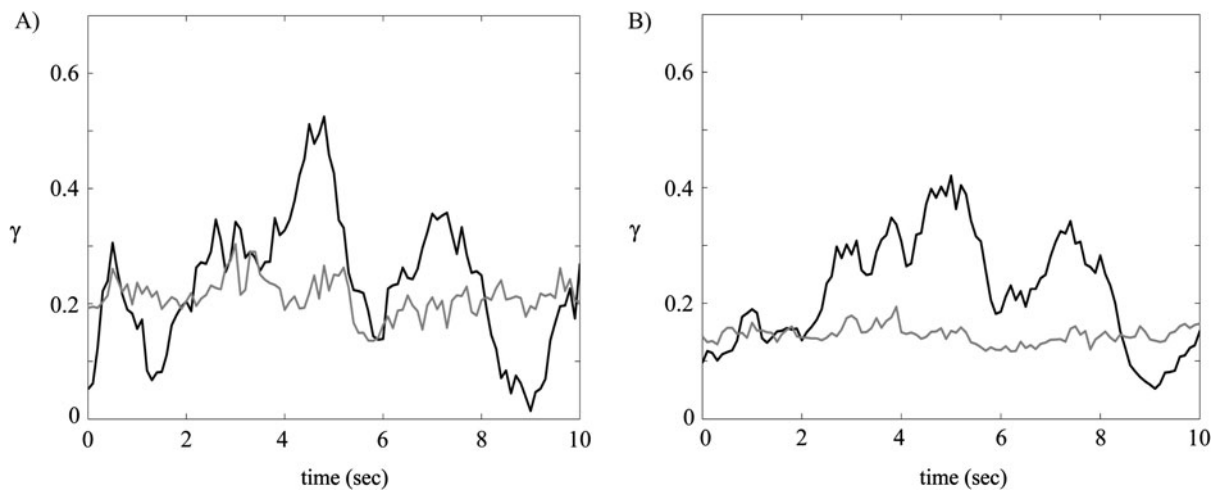


Fig. 4 Dynamics of synchronous activity in time. Black line is the value of the phase-locking index γ computed over a short time-window with duration of 1 s (A) and 1.5 s (B). Each point on the graph of $\gamma(t)$ is the value of γ computed over the

time-window preceding this point. The gray line is the 95% significance level estimate, obtained from surrogate data as described in [65, 66]

on the time-window consisting of N data points. Thus we have a measure of “instantaneous” synchrony, varying between 0 and 1. However, due to the noisy nature and unknown statistical properties of the observed signals, the significance is hard to estimate. One can generate surrogate time-series with the same spectral properties as the original data. This is an important step: time-series are narrow-banded slowly-varying signals and surrogates should be generated accordingly. The comparison of γ obtained from real data with the distribution of γ from the surrogates allows for discrimination between real synchrony and coincidence by chance [66].

Application of this analysis to the data from Parkinsonian patients indicates that γ exhibits substantial variation in time (see Fig. 4). The gray line on the figure is the value of γ obtained from surrogate data (95% confidence level). The value of γ moves above and below significance level as time goes by. Each point in the graph of γ is the phase-locking index computed over the time window of a corresponding length preceding this point, so that γ is not a truly instantaneous measure. And this is the way it’s supposed to be, because synchronization is not an instantaneous phenomenon. Certain value of γ indicates that this is the average level of the phase locking within certain time-interval (1 s in Fig. 4A, 1.5 s in Fig. 4B). As one can see at the figures, the values of γ do depend on the length of this window. This is very natural, for long

time-windows one expects to see less time-variability, for shorter time-windows one has a better temporal resolution and more time-variability as well as less powerful statistics [66]. However, note that for both window length variability of that γ is apparent and the values of γ are in the same range.

One may quantify the average values of γ , or the amount of time the index spends in a certain interval. However, given the high variability of γ with time, it is desirable to develop methods for characterization of this variability; preferably in a way that does not depend (or does not strongly depend) on the time-window length. These ideas are discussed in the next section. In Sect. 5, we will present the results of the application of these ideas to the signals recorded from Parkinsonian brains and will interpret these results.

4 Time-series analysis of observed intermittent synchronized dynamics

As we saw in Fig. 4, the phase-locking index γ computed over short time-windows exhibits high variability. There is a way to study this variability of synchrony in more detail. We see that there is some overall level of phase-locking present in the data. Thus, we can detect the preferred phase difference angle (it is not necessarily zero in this data) and look at whether and how this phase difference angle deviates from its

preferred value at each cycle of oscillations. This is, of course, not an instantaneous measure of synchrony (such a measure is not possible), because we already know that some phase-locking is present. If it were not, then the analysis presented below would not be valid. Thus, one first needs to detect synchronization, for example, by the methods described in the previous section. After it is detected, one can proceed and study synchronization/desynchronization dynamics at each instant of time. These ideas were sketched in [65] and further developed and justified in [69]. Essentially, this is a way to study the dynamics in the phase space away from the synchronous state. This is important because in the weakly synchronized case the system spends most of its time away from the synchronized state. This approach reveals the temporal patterning of synchronous/desynchronous episodes, which cannot be revealed by traditional correlation coefficients, stability properties of the synchronization state, or traditional characteristics of intermittent behavior (distributions of the laminar episodes), etc. [69].

We will describe this approach in discrete time, constructing first return maps for the phase difference. We will also describe it in the context of the Parkinsonian electrophysiology data. After the signals are filtered as explained above and phases are reconstructed, one selects one of the signals (to be specific, let it be LFP) and chooses a check point for the phase of this LFP signal. Again, to make it specific, let this check-point be zero, although this value is clearly not important and can be chosen in different ways. Each time the phase of the LFP signal crosses this check point in a preset direction (either from negative to positive values or vice versa, the particular choice does not matter), the value of the spiking signal phase is recorded. This procedure will generate a set of consecutive values $\{\varphi_{\text{spikes},i}, i = 1, \dots, N$, where N is the number of the checkpoint crossings. Since these values of φ_{spikes} are recorded when $\varphi_{\text{LFP}} = 0$, $\{\varphi_{\text{spikes},i}, i = 1, \dots, N$ is essentially the sequence of the phase difference between signals, measured once in a cycle of LFP oscillation.

Now we can consider a first-return map for the recorded values of the phases $\{\varphi_{\text{spikes},i}, i = 1, \dots, N$. One can plot $\varphi_{\text{spikes},i+1}$ vs. $\varphi_{\text{spikes},i}$ for $i = 1, \dots, N - 1$ (noting that the phase space of our map is a torus, because each coordinate is the phase, defined modulo 2π). A fully phase-locked dynamics would result in a single point on the diagonal $\varphi_{\text{spikes},i+1} =$

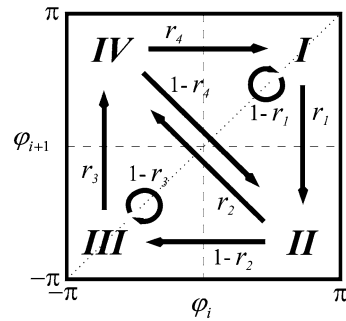


Fig. 5 The diagram of the first-return map of the phases $\{\varphi_{\text{spikes},i}, i = 1, \dots, N$. The arrows describe all possible transitions between four regions of the phase space. The expressions next to the arrows are the rates for each particular type of transitions between the regions. The regions are numbered in a clockwise manner, because the dynamics in the $(\varphi_{\text{spikes},i}, \varphi_{\text{spikes},i+1})$ space mostly follows a clockwise pattern

$\varphi_{\text{spikes},i}$. Completely uncorrelated phases of the signals would result in $(\varphi_{\text{spikes},i}, \varphi_{\text{spikes},i+1})$ space homogeneously filled with the dots. A tendency for predominantly phase-locked dynamics will appear as a cluster of points, centered near the diagonal $\varphi_{\text{spikes},i+1} = \varphi_{\text{spikes},i}$. As was already mentioned above, we apply this analysis only to data with some degree of synchrony to ensure this cluster is present. To allow for uniformity of the analysis, one may determine the center of this cluster and then shift all values of the phases to position the center of the cluster at a point with the coordinates $(\pi/2, \pi/2)$ —the center of the first quadrant. This will eliminate the phase lag value from consideration, but if needed, this value can be recorded and analyzed separately.

To study the temporal dynamics of phase-locking in this framework is to study the dynamics of the first-return map. Consider partitioning of the phase space of the map into four equal regions. Then it is possible to consider and quantify the transitions between these regions (see Fig. 5 for the diagram of the phase space). This partitioning of the phase space implies that a synchronized state is the whole first region. In other words, if the phases of the signals do not deviate from each other by more than $\pi/2$, the signals are considered phase-locked. The evolution outside of the first region represents a desynchronization event. Following [65], to illustrate what it means for the real data we use a short piece of experimentally recorded data, filtered signals and resulting map in Fig. 6.

The value of $\pi/2$ is a compromise value, not too large to exclude large phase deviations, not too small

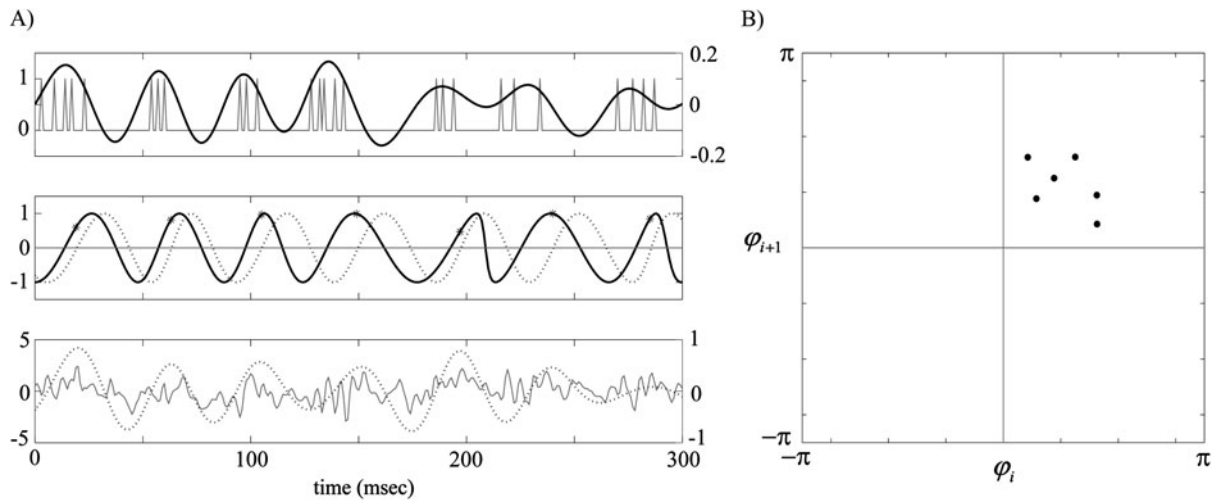


Fig. 6 An example of a short piece of an episode of synchronous LFP and spiking activity in Parkinsonian basal ganglia. **(A)** The upper and the lower panels contain raw and filtered data. The upper panel contains the spikes (gray line) and the spiking signal band-pass filtered to beta-band (black line), the lower panel contains raw LFP signal (gray line), and LFP filtered in the same way (black dotted line). The middle panel has the value of the sine of the phases of filtered spiking and LFP signals. There is clearly visible, but not perfect phase syn-

chrony. *Star* is placed to mark the phase of the filtered spiking signal, when the filtered LFP signal phase crosses zero from below. These marked phases generate the sequence $\{\varphi_{\text{spikes},i}\}$, $i = 1, \dots, N$ used to construct the first-return map shown in part **B**. **(B)** The first-return map $(\varphi_{\text{spikes},i}, \varphi_{\text{spikes},i+1})$ generated from the data at the part **A**. All points are within the first region of the phase space, which corresponds to the phase-locked state. This phase-locking is not perfect, but the phase difference between signals is not changed much during the observation time

either to allow for some substantial fluctuations in the system. The choice of how much tolerance for the phase difference is acceptable ideally should be defined by the function of the considered time-series. One may also perform robustness and sensitivity analysis. The partition into four equal regions has the strong advantage of being symmetric and simple. An extension of these ideas to different partitions is possible, but may be technically challenging. However, even if the partition is too coarse-grained in a functional sense (i.e., the phase-locking should be more precise to perform certain functions), the quantification of the transitions between the regions is still informative and descriptive of the dynamics.

To quantify the dynamics of the map, one can consider four transition rates defined as the number of points in a region, from which the system leaves the region to another specific region, divided by the total number of points in that region. For example, r_1 is the ratio of the number of trajectories escaping the first region for the second region to the number of all points in the first region. While the time-averaged measures of synchrony can characterize whether the synchronization is strong or weak overall, utilization of these

rates lets us explore the dynamics of the phase-locking as a function of time.

The phase space $(\varphi_{\text{spikes},i}, \varphi_{\text{spikes},i+1})$ represents current phase vs. future phase. Therefore, some transitions between quadrants are not possible. For example, there is no transition from the fourth region to itself, because the points in the fourth region are the points with low current phase and high future phase and the future phase is the current phase on the next cycle. Thus the current phase for the next cycle should be high, which limits the transitions to only second and first region. The arrows at Fig. 5 indicate all possible transitions, thus the considered rates r_i provide a fairly complete characterization of how phase-locking breaks down and emerges again in time within this framework.

The rates, besides being a quantitative measure of the dynamics, are related to the durations of the synchronization and desynchronization events. The rate r_1 is related to the average duration of the phase-locked episode (laminar phase in the terminology of intermittency), and thus characterizes the property of the phase-locked state. The average duration of the synchronized phase $\langle l \rangle$ (for an intermittency of differ-

ent types, this quantity scales in a manner specific to each intermittency type) is inversely proportional to r_1 if $\langle l \rangle \sim 1/r_1$. They are equal to each other if $\langle l \rangle$ is measured in the number of iterations of the map (number of cycles of oscillations). The closer r_1 is to 1, the more frequently the synchronized dynamics is interrupted. The transition rates $r_{2,3,4}$ are related to the durations of desynchronizations. Higher values of $r_{2,3,4}$ indicate quicker return to synchronized state and shorter desynchronization episodes, while their low values indicate long desynchronization events.

To further explore the properties of the dynamics in the space $(\varphi_{\text{spikes},i}, \varphi_{\text{spikes},i+1})$, one may compute the relative frequencies of desynchronization events of different durations. In this framework the duration of a desynchronization event is the number of time-steps that system spends away from the first region minus one (because, the point on the map has two coordinates, one of which is a future phase). The desynchronization will always start at the second region. The shortest duration of the desynchronization event corresponds to the shortest path 2-4-1. Since one iteration of the map is usually equals to one cycle of oscillations, this will correspond to the desynchronization length of one cycle of oscillations (in two cycles the phases are back in a locked state). Desynchronization event with duration of two cycles will correspond to the path 2-3-4-1. Longer desynchronization events will have several different paths leading to the same duration.

If transitions between the regions are random and independent of each other, than each new transition will happen with the probability of r_i and the histogram of durations of desynchronization events can be estimated by multiplying the corresponding rates of the transitions for different paths. Thus, to estimate the probability of a desynchronization event of the duration equal to one cycle of oscillations, one needs to consider the shortest path 2-4-1 and the corresponding probability is the product of transition rates $r_2 r_4$ along the path. Duration of two cycles is possible with 2-3-4-1, the corresponding probability is $r_2 r_3 r_4$. Two different paths are possible for three-cycle duration: 2-4-2-4-1 and 2-3-3-4-1; the corresponding probability is $r_2 \cdot (1 - r_4) \cdot r_2 \cdot r_4 + (1 - r_2) \cdot (1 - r_3) \cdot r_3 \cdot r_4$. Clearly, these probabilities can be computed for any duration. In the case of Parkinsonian data, the transitions are close to independent, so that such estimation of durations gives results close to the one obtained from the map directly [65]. In general, while some sys-

tems may allow for such an approximation, some lack this property [69].

We would like to note that although we use this approach to study neural synchronization in the Parkinsonian brain, it may be applicable to different models and real systems and data [69]. It provides a quantitative description of how synchrony develops in time and thus may be relevant in many biological and medical applications. Living systems are highly adaptable to the changes in the environment and thus are expected to be variable to be controllable. Therefore synchronization phenomena in many living systems may be expected to be variable and synchronization if averaged over long-time intervals may be quite weak. Thus some traditional measures of synchrony, like indices of phase-coherence (in the time-series analysis approach) and stability properties/Lyapunov exponent of the synchronized state (in the phase-space approach) do not necessarily tell much about weakly synchronized dynamics (the system spends most of the time in the phase space away from the synchronized state). The analysis of the fine temporal structure of the phase-locking described above may be very useful in the analysis of this type of variable dynamics. It also has the potential to assist in studies of how such important factors as noise, type of oscillators and strength and topology of network connectivity affect not only the average synchrony, but its dynamics as well.

5 Fine temporal structure of intermittent synchronization in Parkinsonian brain

Since we study the episodes of oscillatory activity with a tendency for phase-locking, the first-return map should have a cluster of points centered near the diagonal. This is clearly visible in the example presented in Fig. 7. A piece of an oscillatory synchronous episode of data recorded in a patient was processed as discussed in the previous sections. The cluster has a relatively large size, which means the synchrony is not perfect. Most of the time the difference between the phases of LFP and spikes does not experience very large variations, yet it is not perfectly constant either. The same relationship is expected for the cellular and synaptic activity underlying extracellular spiking and LFP signals, respectively.

It is important to properly characterize the dynamics and understand the mechanisms of this kind of activity. The dynamics of the maps like those on Fig. 7

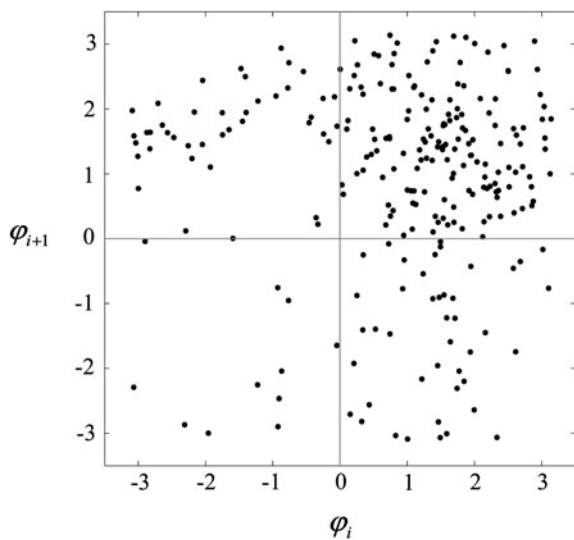


Fig. 7 First return map obtained from experimentally recorded extracellular units and LFPs from the subthalamic nucleus of a Parkinsonian patient. The dynamics is not perfectly synchronous, as evidenced by a scatter of points, however, the tendency for phase-locking is visible: there is a higher density of points in the first (synchronized) region

can be quantified as in the previous section. The transition rates and durations of desynchronization events not only describe the fine temporal structure of the dynamics, but also provide quantitative characteristics of the organization of the phase space to be used in comparison with modeling studies, as we will discuss in the next section.

Average values for transition rates for a population of Parkinsonian patients have been computed in [65] (and are presented at Fig. 8). The transition rate r_1 is of the order of 0.3–0.4. This means the phase-locking in the basal ganglia is interrupted by desynchronized dynamics every three periods of oscillations on average. The rates r_2 , r_3 , and r_4 are of the order of 0.6–0.7. Relatively high values of these three transition rates indicate the tendency for a quick return to the phase-locked state. Different data inclusion criteria and different averaging methods yield similar results. Thus the transition rates appear to be relatively robust characteristics of synchronization/desynchronization dynamics.

The computation of the histogram of durations of desynchronization events (Fig. 9) naturally agrees with these observations of rates (Fig. 8). The most dominant duration of desynchronization is the shortest one. It is more frequent than the next two frequent by

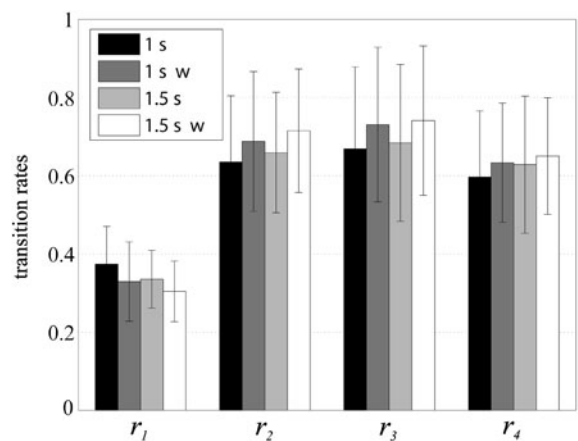


Fig. 8 The transition rates r_1, r_2, r_3, r_4 obtained from data recorded in a sample of Parkinsonian patients. Average and standard deviation are shown. Four different bars for each transition rate are the values of that rate computed in different ways. Different selection criteria of synchronized episodes (different length of duration of the running window to compute the phase-locking index) are represented by *black/dark gray* and *light gray/white bars*. Different averaging procedures (arithmetic mean value and weighted mean computed with weights proportional to the length of each individual episode of the data) are represented by *black/light gray* and *dark gray/white bars*. The rates obtained with different methods are only slightly different from each other. Overall, the rates are not very sensitive to the data selection criteria and averaging technique

a factor of 3 or so. The distribution of durations tends to decrease with the increase of duration length. Similarly to the case with the rates, the results do not depend on the kind of averaging procedure qualitatively. A particular value of the rate depends on many factors, however the overall robustness of the rates and histogram of durations suggest that the dominance of the short desynchronization does not depend on the particular details of how the fine temporal structure of the phase-locking is studied.

Calculation of durations from the rates under the assumption of independent transitions yields very similar, although not identical results [65]. Therefore the transitions between different parts of the phase space weakly depend on the past dynamics.

In general the same level of synchrony can be supported by different details of synchronization/desynchronization dynamics. In two extremes, the moderate phase-locking strength may be achieved by a relatively large number of short desynchronization events or by a moderate number of long desynchronization events. The discussed work shows that basal ganglia networks in Parkinson's disease are apparently closer

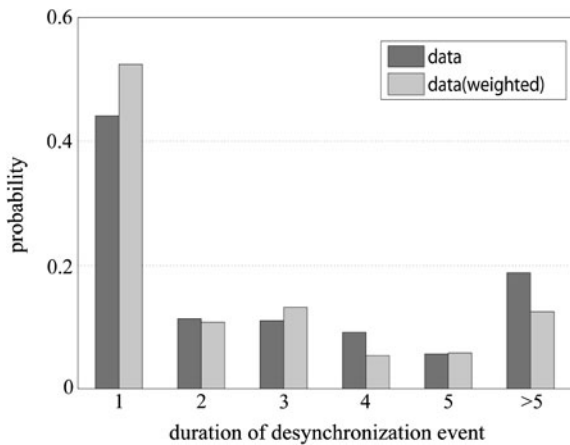


Fig. 9 The histogram of the durations of desynchronization events. The *light bars* correspond to computing the frequencies of duration within each data episode and averaging them across the episode (this corresponds to the arithmetical mean rates in Fig. 8). The *dark bars* correspond to the averaging the frequencies of desynchronization event durations for all episodes together (this corresponds to the weighted average rates in Fig. 8, each data episode makes an impact proportional to its length). All durations of six cycles of oscillations and longer are pulled together in “>5” group. Similar to the rates (Fig. 8), different averaging techniques give values, which are different only slightly; overall tendency for the largest first bin of the histogram is preserved

to the former extreme. The signals go out of phase for just one cycle of oscillations more often than for two or a larger number of cycles. The predominance of short, yet relatively frequent desynchronization events may have certain implications for the functional aspects of basal ganglia physiology in PD, which we discuss in the Sect. 7.

6 Modeling intermittent synchrony in basal ganglia circuits

6.1 Modeling approach

Quite a lot is known about the biophysical properties of cells in basal ganglia nuclei [34, 35]. Cellular physiology of different basal ganglia nuclei has been studied using a variety of techniques from voltage clamp studies to in vivo recordings of neural activity and its responses to various stimulations (electrical or chemical). One of the prominent models of the basal ganglia circuitry is the conductance-based model of subthalamo-pallidal circuits of basal ganglia developed by Terman and colleagues [70]. While the model

is clearly limited to these local circuits, there are various indications that the model captures the rich repertoire of Parkinsonian rhythmicity, recorded in these circuits in Parkinsonian patients and animals. In addition, this kind of approach appears to adequately reproduce the experimentally studied mechanisms of this rhythmicity resulting from sequences of recurrent excitation and inhibition in subthalamo-pallidal networks [33, 71].

The individual GPe and STN neurons in this model are described by single-compartment conductance-based models. Both model STN and GPe neurons involve the same currents; they exhibit different firing properties due to their parameters (reflecting the properties of membrane currents and degree to which they are expressed in the membranes). The model has standard sodium, potassium and leak currents, low threshold T-type Ca^{2+} -current, high-threshold Ca^{2+} current, and Ca^{2+} -activated voltage-independent afterhyperpolarization K^+ -current, which are responsible for the oscillatory properties of the cells. The equation for the membrane potential is

$$C \frac{dV}{dt} = -I_L - I_K - I_{Na} - I_T - I_{Ca} - I_{AHP} - I_{syn} + I_{app},$$

where leak current is $I_L = g_L(V - V_L)$, fast potassium and sodium currents are $I_K = g_K n^4(V - V_K)$ and $I_{Na} = g_{Na} m_{\infty}^3(V)h(V - V_{Na})$, calcium currents are $I_T = g_T a_{\infty}^3(V)b_{\infty}^2(r)(V - V_{Ca})$ and $I_{Ca} = g_{Ca} s_{\infty}^2(V)(V - V_{Ca})$, and “afterhyperpolarization” current is $I_{AHP} = g_{AHP}([Ca]/([Ca] + k_1))(V - V_K)$. $[Ca]$ is concentration of intracellular Ca^{2+} ions, and the equation of the calcium balance is

$$d[Ca]/dt = \varepsilon(-I_{Ca} - I_T - k_{Ca}[Ca]).$$

n, h and r are gating variables described by first-order kinetic equations of this type:

$$dx/dt = (x_{\infty}(V) - x)/\tau(V),$$

and m_{∞}, a_{∞} and s_{∞} are instantaneous voltage-dependent gating variables. Thus each model neuron is a five-dimensional nonlinear dynamical system.

Synaptic input from other cells is represented by I_{syn} . The model consists of a chain of STN neurons and chain of GPe neurons. In the case of the modeling studies considered here, each STN neuron projects to a corresponding GPe neuron, each GPe neuron projects to the corresponding STN neuron and

both of its two nearest neighbors. Applied current to GPe neurons is a constant current, which, in particular, takes into account striatal inhibitory input to external pallidum (we will explain below, why variation of this parameter in the model is reflective of the normal/Parkinsonian transition). Overall, the architecture of the network is in realistic correspondence with the anatomy of STN-GP circuits [72–74], although some finer details of the connectivity are either not represented in the model or not known at all. The synaptic connections (excitatory glutamatergic and inhibitory GABAergic synapses) are modeled by 1st-order kinetic equations for the fraction of activated synaptic channels:

$$\frac{ds}{dt} = \alpha H_\infty(V_{\text{presyn}} - \theta_g)(1 - s) - \beta s,$$

where H_∞ is a sigmoidal function. The synaptic current is given by $I_{\text{syn}} = g_{\text{syn}}(V - V_{\text{syn}}) \sum_j s_j$, where summation is over s-variables from all neurons projecting to a given neuron. The model does not explicitly consider rhythmic inputs to pallido-subthalamic circuits from cortex and other structures. These inputs may play some role in the dynamics. However, even if the pathological rhythmicity also comes from outside, the circuit still should have relevant oscillatory properties to be engaged in interaction with inputs.

Experimentally recorded extracellular spikes in STN can be modeled by the spikes obtained from the model transmembrane potential $V(t)$. However, LFP are not explicitly represented in the model. LFP are primarily generated by synaptic potentials and thus reflect incoming and local processing activity [75, 76]. Similarly to the cortex, LFP recorded in different parts of basal ganglia are of synaptic origin and are relatively locally generated [27, 29, 53]. LFP are not as local as the extracellular spikes signal [29], but they are generated in a vicinity of the recording electrode. The existence of local connections within STN is very unlikely [77]. Thus the model STN LFP should have its origin in pallido-subthalamic synaptic transmission that is defined by the activity of the synapses from GPe to STN cells.

Model LFP can be computed as the weighted sum of synaptic activity in a relatively small area of the model network. Synaptic input to the i th STN neuron is $I_{\text{GS}}^i = g_{\text{GS}}(V^i - V_{\text{syn}}) \sum_{j=i-1}^{i+1} s_j$. Then model STN LFP at this location is

$$\text{LFP}^i = I_{\text{GS}}^i + w^*(I_{\text{GS}}^{i-1} + I_{\text{GS}}^{i+1}),$$

where w is the weight representing the impact of more remote synaptic activity on the voltage of LFP at a given location. Inclusion of an additional term, $(I_{\text{GS}}^{i-2} + I_{\text{GS}}^{i+2})$, with small weight sw will incorporate a larger area into LFP computation. However, in the numerical studies considered below this term did not substantially change the outcome of the synchronization analysis.

This kind of model allows one to easily vary any parameter, independently of other factors to study the model dynamics and its mechanisms. Experimental approaches appear to be quite limited here. In vitro experiments would unavoidably damage the networks, while in vivo experiments would be hampered by a restricted set of dopaminergic states and other limitations. Modeling allows one to avoid these constraints.

6.2 Model dynamics

Basal ganglia synapses are modulated by dopamine and hence, the dopaminergic degeneration in Parkinson's disease leads to the modulation of synaptic strength. For many basal ganglia synapses this results in an increase of the strength of synaptic connections, because dopamine tends to suppress them. Dopamine is known to act on presynaptic D2 receptors at striato-pallidal synapses reducing GABA release in GPe [78–80]. In perhaps a similar manner, dopaminergic action in STN inhibits GABA release, in particular, from synapses from neurons originating in GPe [81–86]. These experimental results are reflected by altered values [87] of two parameters of the model pallido-subthalamic network: synaptic strength of inhibitory GPe-STN projections, g_{syn} , and the applied current term in the GPe model neuron, I_{app} , which represents effect of inhibitory striatopallidal synapses.

For moderately large values of these parameters the model generates dynamics which shares a lot of similarity with the experimentally observed dynamics. The dependence of the phase-locking index computed over short time windows exhibits substantial variations (Fig. 10) as the experimentally computed computer index does (Fig. 4). The first-return maps for the phase differences in the model for some parameter values (Fig. 11) are similar to the maps obtained from experimental data (Fig. 7). Similar to the experiment, the model dynamics spends most of the time in the first region, making numerous short excursions from it. Importantly, this is not only visual similarity

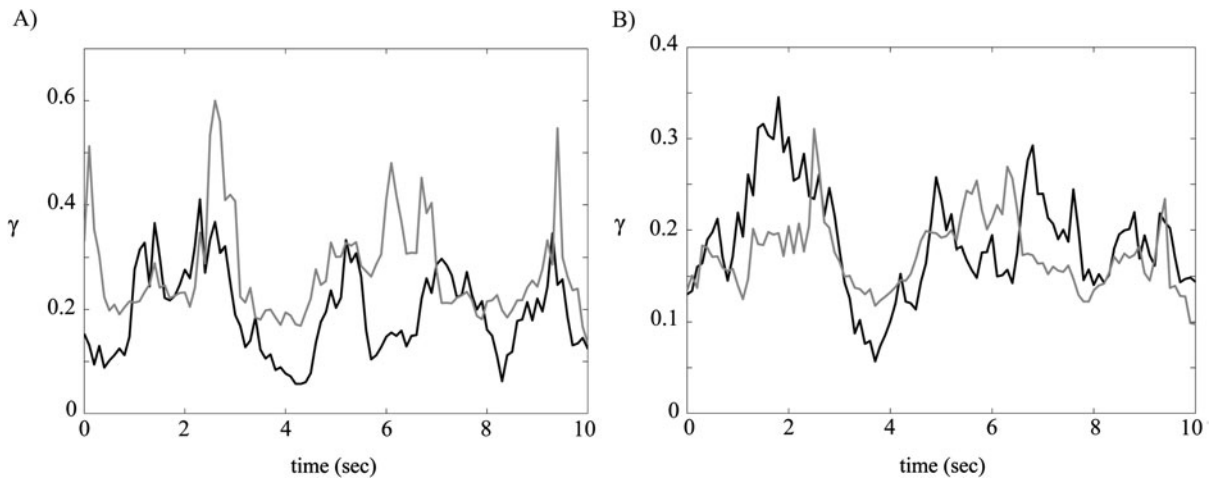


Fig. 10 Dynamics of model's synchronous activity in time. The phase-locking index γ is computed for model spiking and LFP in the same way as it was computed for the real data in Fig. 4. The duration of the time-window used for computation of γ is 1 s (A) and 1.5 s (B). The gray line is the 95% significance level estimate, obtained from surrogate data

of pictures. The comparison of the rates r_1, r_2, r_3, r_4 obtained from the model, indicate that all four approximate the experimental rates very well [87]. Therefore, not only does the synchrony fluctuate in the same way in the model and the experiment, but the phase space of the model and of the real network is organized in a quantitatively similar manner. The distributions of durations of desynchronization events in the model and in the experiment are similar too. Thus, the mechanisms and assumptions of the model network are sufficient to generate the intermittency of synchrony observed in the experiments.

In [87] the model parameters were varied to explore the dynamics in the parameter space (g_{syn}, I_{app}) and to determine if there exists a parameter domain where the model dynamics exhibit intermittent phase-locking similar to that observed in experiment. As we discussed above, the use of an average phase-locking index is not sufficiently constraining. However, if transition rates r_1, r_2, r_3, r_4 are used to compare the dynamics, not only the average synchrony, but also the organization of the phase space will be compared. This ensures greater equivalency of the model and the real system. Of course, there are many characteristics of dynamics which might be used for comparison. The rates r_1, r_2, r_3, r_4 appear to be advantageous because they characterize features of the dynamics which are relevant to the symptoms of the disease. This similarity of the rates will also lead to similarity of the distribution of durations of desynchronization events, be-

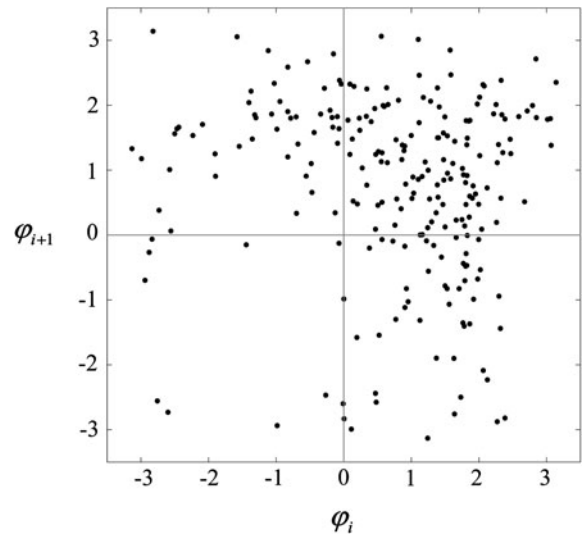


Fig. 11 First return map obtained from the model-generated spiking and LFP signals. Compare with the Fig. 7

cause, as we discussed, they are relatively closely related for this Parkinsonian data.

The results of this comparison are presented in Fig. 12. This is (g_{syn}, I_{app}) parameter space. The circles indicate the number of principle components, computed in the principle component analysis (PCA), needed to capture 80% variation of the observed dynamics. Thus these circles indicate the overall coherence in the model network. The right lower corner of this diagram (higher g_{syn} and lower I_{app}) corresponds

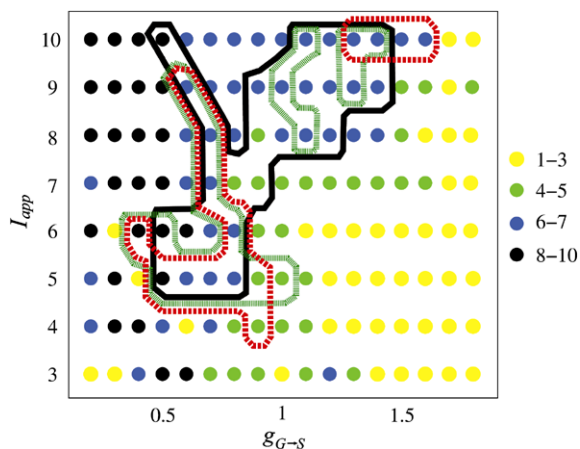


Fig. 12 The comparison of the model with experimental dynamics in (g_{syn}, I_{app}) parameter space (follows [87]). The circles indicate the number of principle components capturing the dynamics computed from for the slow variable r of all model STN cells (r is the slow variable, and thus it is more appropriate for the study of synchrony in the slow bursting beta-frequency band, rather than fast variables related to spikes). The lines represent the contours of the parameter domains, where all four model rates r_i are within 0.7 SD of the experimental rates. Solid, dotted, and dashed lines correspond to different values of the weights used to compute model LFP. Note that I_{app} is positive in the model (as it was originally developed in [70]), thus the increase of inhibition of GPe by striatum, induced by the lack of dopamine, is represented by a decrease in I_{app}

to lower dopamine levels (extreme Parkinsonian state) while the higher dopamine levels (more healthy state) are closer to the upper left corner. The right lower corner of the parameter plane is a region of highly correlated activity (there are a small number of principle components) while the left upper corner exhibits uncorrelated dynamics. This is, perhaps, not a surprising outcome, as the stronger coupling is expected to lead to more synchronous dynamics. However, given the experimental data available, one can match them with the modeling output to see where the region with realistic dynamics is located (if it exists at all) and how large it is.

This region where the model activity is “dynamically” similar to the activity in Parkinson’s disease is situated in between the extreme cases of incoherent and very synchronous dynamics. Its exact location and form depend on how strong the similarity requirements are and on model parameters. In particular, it depends on how the model LFPs are computed, but qualitatively these do not change its location. The weights w used in the model LFP computation are not

exactly known. However even if they are varied in a relatively broad range, the results are not much different qualitatively (Fig. 12). Therefore the location of the region of realistic Parkinsonian synchrony is robust and is on the boundary between synchronized and nonsynchronized dynamics in the network.

There are many more dopamine-modulated parameters in the basal ganglia than we consider here. For example, excitatory projections from STN to GPe are suppressed by dopaminergic action both presynaptically through D2-like receptors and postsynaptically through D4-like receptors [88]. Dopamine also has a tendency to depolarize STN cells [89, 90], which may increase responsiveness of STN cells to synaptic input, which, in turn, facilitates a more connected network. Overall, dopamine depletion seems to make the elements of the basal ganglia circuitry more functionally connected (e.g., [35]). However, if the lack of dopamine leads to even stronger functional connections, we would not expect the results to change much. The important message of the numerical studies described here is that there is a broad region of realistic dynamics which exists for moderate values of connection strengths in the basal ganglia network.

The modeling considered above is one of the ways to study the mechanisms behind the observed intermittent dynamics from the nonlinear dynamics perspective. So far the modeling signifies the role of appropriate coupling strength. The complex interactions of the slow dynamical variables (slow, calcium-driven dynamics) may also play a significant role [91]. However the question of what defines the nature of the observed intermittency is still open and the problem is very challenging, in particular because the structure of the desynchronized events is defined by the organization of the phase space beyond the synchronization manifold and thus is not universal (see [69] for a discussion of this issue).

The model network considered here cannot capture all the brain networks with beta-band oscillations. However, in general the lack of dopamine in basal ganglia circuits apparently promotes the strength and synchrony of these oscillations (see multiple references in Sect. 2). So, if the dynamics of oscillations in different parts of cortico-basal ganglia-thalamic networks in response to dopamine is consistent, the results of the study of intermittent beta-band synchronous oscillation in one node of these networks (such as STN) may be quite typical for these networks as a whole.

7 Dynamical state of Parkinsonian brain

Time-series analysis has revealed the intermittent nature of brain activity in Parkinson's disease and specifically the fine temporal structure of beta oscillations. The modeling studies suggest what may induce this variability of synchrony. In general, several factors might contribute to the variability, including short-term plasticity in basal ganglia networks, noise and fluctuating inputs from other parts of the nervous system. However, the modeling suggests that this variability may arise intrinsically in the basal ganglia networks due to a moderate increase in connectivity between network elements (an increase which is expected to result from the dopaminergic degeneration).

We conjecture that this may be a generic situation. There are experimental examples of transient synchrony in the brain, needed for physiologically significant events (e.g. [6, 7, 10]) and transient dynamics would be very reasonable from theoretical standpoint [92, 93]. In these examples transient synchrony is recruited to achieve a particular physiological effect. In our case, in Parkinson's disease even at rest the synchrony is easy to form. This may be the result of the fact that synchronized oscillations have some healthy function too. It is known that synchronous oscillations in the beta band are related to the preparation of a new movement or to maintenance of the current motor set [55].

Taking this into account together with the modeling results, one may suggest that moving further away from the boundary of the synchronization region into the region of nonsynchronized dynamics, the network may enter a more healthy state [87]. In that state synchrony may be possible only if other parts of neural system (transiently) bring it close to the boundary. Thus healthy networks may exist functionally close to the boundary area too, so that synchrony of beta-band oscillations may be generated when needed (to prepare for a new movement or to maintain motor status quo). In a pathological state, the coupling in the network is stronger due to the lack of dopamine. This moves the network towards the more synchronized state and the transient synchronous patterns become more prevalent and harder to break, which would prevent the execution of the new movement.

In other words, the intermittent synchrony which we observe in the Parkinsonian state may be a result of a propensity of basal ganglia circuits to be engaged

in the brief synchronized episodes of activity needed for movement control. The low-dopamine state with stronger coupling and stronger common input may result in a partial suppression of this very transient (and hard-to-detect) character of neuronal dynamics, favoring only short desynchronization events, which interrupt mostly synchronous episodes [65].

In connection with this consideration, it will be interesting to see if another prominent type of pathological synchronous oscillation in Parkinson's disease—tremor oscillations—are pathologically augmented traces of some kind of normal oscillatory function. Parkinsonian tremor also presents intermittent synchronous dynamics [66, 67, 94], so their origin remains to be investigated.

Overall, operation on the boundary of synchronization may potentially have some important advantages as we have discussed in [87]. Very robust, perfectly synchronous oscillations may be hard to modulate, therefore they may be less efficient in transmitting information which is the major function of nervous system. Operation at the edge of synchrony would yield the creation and disappearance of unstable synchronized clusters possible without much expense, allowing for easy formation and dissolution of transient neuronal assemblies. In turn, this would either directly contribute to a fluid and timely sequence of movements or facilitate information transmission through the oscillations. Thus pathological and healthy oscillations may be related.

The intermittent nature of the synchronous dynamics in Parkinsonian basal ganglia may also have some important ramifications for Parkinson's disease treatment. At the present time there is no cure for Parkinson's disease and pharmacological treatment of symptoms usually leads to substantial side-effects in the long run. Thus there is a substantial interest in basal ganglia DBS in Parkinson's disease. STN DBS is the most frequent surgical procedure in Parkinson's disease. This "classical" DBS requires delivering large amplitude high-frequency pulses, which are probably so strong that they simply override the pathological beta-band synchronized oscillations. This is sub-optimal procedure and it has multiple side effects. This leads to interest in effective adaptive control strategies to suppress the pathological rhythmicity. Therefore it is important to understand the nature of the dynamics one wishes to suppress, that is the dynamical nature on these synchronized oscillations. The approach considered here may provide a way to this understanding.

Previous modeling studies have presented examples of how delayed nonlinear feedback may destabilize synchronous oscillations [95–97]. However, currently we still await an experimental realization of these adaptive DBS techniques. One of the problems may be the complex nature of intermittent partially synchronous beta-band oscillations in Parkinson's disease. As we see the real pathological state is not one of perfect synchrony, but rather exhibits a complicated weakly synchronized and highly intermittent dynamics. While we can characterize it and can generate it in the model, its mechanisms in a mathematical sense are still far from being understood. These mechanisms must define how the presumably desynchronizing stimulation will act on a dynamics which is not fully synchronous to begin with. The models considered here may assist in the study of this problem.

Acknowledgements Supported by the National Institutes of Health grant R01NS067200 (NSF/NIH CRCNS program).

References

1. Abarbanel, H.D.I., et al.: Synchronization in neural networks. *Phys. Usp.* **39**, 337–362 (1996)
2. Rabinovich, M.I., et al.: Dynamical principles in neuroscience. *Rev. Mod. Phys.* **78**(4), 1213–1265 (2006)
3. Izhikevich, E.M.: *Dynamical Systems in Neuroscience: The Geometry of Excitability and Bursting*. The MIT Press, Cambridge (2007)
4. Ermentrout, G.B., Terman, D.H.: *Mathematical Foundations of Neuroscience*. Springer, New York (2010)
5. Pikovsky, A., Rosenblum, M., Kurths, J.: *Synchronization: A Universal Concept in Nonlinear Sciences*. Cambridge University Press, Cambridge (2001)
6. Engel, A.K., Fries, P., Singer, W.: Dynamic predictions: oscillations and synchrony in top-down processing. *Nat. Rev., Neurosci.* **2**(10), 704–716 (2001)
7. Buzsaki, G., Draguhn, A.: Neuronal oscillations in cortical networks. *Science* **304**(5679), 1926–1929 (2004)
8. Uhlhaas, P.J., et al.: Neural synchrony and the development of cortical networks. *Trends Cogn. Sci.* **14**(2), 72–80 (2010)
9. Fell, J., Axmacher, N.: The role of phase synchronization in memory processes. *Nat. Rev., Neurosci.* **12**(2), 105–118 (2011)
10. Sanes, J.N., Donoghue, J.P.: Oscillations in local field potentials of the primate motor cortex during voluntary movement. *Proc. Natl. Acad. Sci. USA* **90**(10), 4470–4474 (1993)
11. Murthy, V.N., Fetz, E.E.: Oscillatory activity in sensorimotor cortex of awake monkeys: synchronization of local field potentials and relation to behavior. *J. Neurophysiol.* **76**(6), 3949–3967 (1996)
12. Baker, S.N., et al.: The role of synchrony and oscillations in the motor output. *Exp. Brain Res.* **128**(1–2), 109–117 (1999)
13. Schnitzler, A., Gross, J.: Normal and pathological oscillatory communication in the brain. *Nat. Rev., Neurosci.* **6**(4), 285–296 (2005)
14. Uhlhaas, P.J., Singer, W.: Neural synchrony in brain disorders: relevance for cognitive dysfunctions and pathophysiology. *Neuron* **52**(1), 155–168 (2006)
15. Uhlhaas, P.J., Singer, W.: Abnormal neural oscillations and synchrony in schizophrenia. *Nat. Rev., Neurosci.* **11**(2), 100–113 (2010)
16. Le Van Quyen, M., Bragin, A.: Analysis of dynamic brain oscillations: methodological advances. *Trends Neurosci.* **30**(7), 365–373 (2007)
17. Rivlin-Etzion, M., et al.: Basal ganglia oscillations and pathophysiology of movement disorders. *Curr. Opin. Neurobiol.* **16**(6), 629–637 (2006)
18. Hutchison, W.D., et al.: Neuronal oscillations in the basal ganglia and movement disorders: evidence from whole animal and human recordings. *J. Neurosci.* **24**(42), 9240–9243 (2004)
19. Boraud, T., et al.: Oscillations in the basal ganglia: The good, the bad, and the unexpected. In: Bolam, J.P., Ingham, C.A., Magill, P.J. (eds.) *The Basal Ganglia VIII*. Springer, New York (2005)
20. Gatev, P., Darbin, O., Wichmann, T.: Oscillations in the basal ganglia under normal conditions and in movement disorders. *Mov. Disord.* **21**(10), 1566–1577 (2006)
21. Hammond, C., Bergman, H., Brown, P.: Pathological synchronization in Parkinson's disease: networks, models and treatments. *Trends Neurosci.* **30**(7), 357–364 (2007)
22. Bergman, H., et al.: Physiological aspects of information processing in the basal ganglia of normal and Parkinsonian primates. *Trends Neurosci.* **21**(1), 32–38 (1998)
23. Goldberg, J.A., et al.: Enhanced synchrony among primary motor cortex neurons in the 1-methyl-4-phenyl-1,2,3,6-tetrahydropyridine primate model of Parkinson's disease. *J. Neurosci.* **22**(11), 4639–4653 (2002)
24. Soares, J., et al.: Role of external pallidal segment in primate Parkinsonism: comparison of the effects of 1-methyl-4-phenyl-1,2,3,6-tetrahydropyridine-induced Parkinsonism and lesions of the external pallidal segment. *J. Neurosci.* **24**(29), 6417–6426 (2004)
25. Costa, R.M., et al.: Rapid alterations in corticostriatal ensemble coordination during acute dopamine-dependent motor dysfunction. *Neuron* **52**(2), 359–369 (2006)
26. Sharott, A., et al.: Directional analysis of coherent oscillatory field potentials in the cerebral cortex and basal ganglia of the rat. *J. Physiol.* **562**(Pt 3), 951–963 (2005)
27. Magill, P.J., et al.: Brain state-dependency of coherent oscillatory activity in the cerebral cortex and basal ganglia of the rat. *J. Neurophysiol.* **92**(4), 2122–2136 (2004)
28. Magill, P.J., et al.: Changes in functional connectivity within the rat striatopallidal axis during global brain activation in vivo. *J. Neurosci.* **26**(23), 6318–6329 (2006)
29. Goldberg, J.A., et al.: Spike synchronization in the cortex/basal-ganglia networks of Parkinsonian primates reflects global dynamics of the local field potentials. *J. Neurosci.* **24**(26), 6003–6010 (2004)

30. Fogelson, N., et al.: Different functional loops between cerebral cortex and the subthalamic area in Parkinson's disease. *Cereb. Cortex* **16**(1), 64–75 (2006)
31. Lalo, E., et al.: Patterns of bidirectional communication between cortex and basal ganglia during movement in patients with Parkinson disease. *J. Neurosci.* **28**(12), 3008–3016 (2008)
32. Plenzy, D., Kital, S.T.: A basal ganglia pacemaker formed by the subthalamic nucleus and external globus pallidus. *Nature* **400**(6745), 677–682 (1999)
33. Bevan, M.D., et al.: Move to the rhythm: oscillations in the subthalamic nucleus-external globus pallidus network. *Trends Neurosci.* **25**(10), 525–531 (2002)
34. Surmeier, D.J., Mercer, J.N., Chan, C.S.: Autonomous pacemakers in the basal ganglia: who needs excitatory synapses anyway? *Curr. Opin. Neurobiol.* **15**(3), 312–318 (2005)
35. Bevan, M.D., Atherton, J.F., Baufretton, J.: Cellular principles underlying normal and pathological activity in the subthalamic nucleus. *Curr. Opin. Neurobiol.* **16**(6), 621–628 (2006)
36. Cassidy, M., et al.: Movement-related changes in synchronization in the human basal ganglia. *Brain* **125**(Pt 6), 1235–1246 (2002)
37. Levy, R., et al.: Dependence of subthalamic nucleus oscillations on movement and dopamine in Parkinson's disease. *Brain* **125**(Pt 6), 1196–1209 (2002)
38. Kuhn, A.A., et al.: Event-related beta desynchronization in human subthalamic nucleus correlates with motor performance. *Brain* **127**(Pt 4), 735–746 (2004)
39. Amirnovin, R., et al.: Visually guided movements suppress subthalamic oscillations in Parkinson's disease patients. *J. Neurosci.* **24**(50), 11302–11306 (2004)
40. Brown, P., et al.: Dopamine dependency of oscillations between subthalamic nucleus and pallidum in Parkinson's disease. *J. Neurosci.* **21**(3), 1033–1108 (2001)
41. Priori, A., et al.: Rhythm-specific pharmacological modulation of subthalamic activity in Parkinson's disease. *Exp. Neurol.* **189**(2), 369–379 (2004)
42. Williams, D., et al.: Dopamine-dependent changes in the functional connectivity between basal ganglia and cerebral cortex in humans. *Brain* **125**(Pt 7), 1558–1569 (2002)
43. Levy, R., et al.: Effects of apomorphine on subthalamic nucleus and globus pallidus internus neurons in patients with Parkinson's disease. *J. Neurophysiol.* **86**(1), 249–260 (2001)
44. Sharott, A., et al.: Dopamine depletion increases the power and coherence of beta-oscillations in the cerebral cortex and subthalamic nucleus of the awake rat. *Eur. J. Neurosci.* **21**(5), 1413–1422 (2005)
45. Silberstein, P., et al.: Cortico-cortical coupling in Parkinson's disease and its modulation by therapy. *Brain* **128**(Pt 6), 1277–1291 (2005)
46. Kuhn, A.A., et al.: Frequency-specific effects of stimulation of the subthalamic area in treated Parkinson's disease patients. *NeuroReport* **20**(11), 975–978 (2009)
47. Weinberger, M., et al.: Beta oscillatory activity in the subthalamic nucleus and its relation to dopaminergic response in Parkinson's disease. *J. Neurophysiol.* **96**(6), 3248–3256 (2006)
48. Marceglia, S., et al.: Dopamine-dependent non-linear correlation between subthalamic rhythms in Parkinson's disease. *J. Physiol.* **571**(Pt 3), 579–591 (2006)
49. Dejean, C., et al.: Dynamic changes in the cortex-basal ganglia network after dopamine depletion in the rat. *J. Neurophysiol.* **100**(1), 385–396 (2008)
50. Wingeier, B., et al.: Intra-operative STN DBS attenuates the prominent beta rhythm in the STN in Parkinson's disease. *Exp. Neurol.* **197**(1), 244–251 (2006)
51. Kuhn, A.A., et al.: High-frequency stimulation of the subthalamic nucleus suppresses oscillatory beta activity in patients with Parkinson's disease in parallel with improvement in motor performance. *J. Neurosci.* **28**(24), 6165–6173 (2008)
52. Eusebio, A., et al.: Deep brain stimulation can suppress pathological synchronisation in Parkinsonian patients. *J. Neurol., Neurosurg. Psychiatry* **82**(5), 569–573 (2011)
53. Brown, P., Williams, D.: Basal ganglia local field potential activity: character and functional significance in the human. *Clin. Neurophysiol.* **116**(11), 2510–2519 (2005)
54. Brown, P.: Abnormal oscillatory synchronisation in the motor system leads to impaired movement. *Curr. Opin. Neurobiol.* **17**(6), 656–664 (2007)
55. Engel, A.K., Fries, P.: Beta-band oscillations—signalling the status quo? *Curr. Opin. Neurobiol.* **20**(2), 156–165 (2010)
56. Leblois, A., et al.: Late emergence of synchronized oscillatory activity in the pallidum during progressive Parkinsonism. *Eur. J. Neurosci.* **26**(6), 1701–1713 (2007)
57. Mallet, N., et al.: Disrupted dopamine transmission and the emergence of exaggerated beta oscillations in subthalamic nucleus and cerebral cortex. *J. Neurosci.* **28**(18), 4795–4806 (2008)
58. Chen, C.C., et al.: Excessive synchronization of basal ganglia neurons at 20 Hz slows movement in Parkinson's disease. *Exp. Neurol.* **205**(1), 2142–2151 (2007)
59. Pogosyan, A., et al.: Boosting cortical activity at Beta-band frequencies slows movement in humans. *Curr. Biol.* **19**(19), 1637–1641 (2009)
60. Montgomery, E.B.: Basal ganglia physiology and pathophysiology: a reappraisal. *Parkinsonism Relat. Disord.* **13**(8), 455–465 (2007)
61. Gale, J.T., et al.: From symphony to cacophony: pathophysiology of the human basal ganglia in Parkinson disease. *Neurosci. Biobehav. Rev.* **32**(3), 378–387 (2008)
62. Gradinaru, V., et al.: Optical deconstruction of Parkinsonian neural circuitry. *Science* **324**(5925), 354–359 (2009)
63. Hutchison, W.D., Dostrovsky, J.O., Lozano, A.M.: Movement disorders surgery: microelectrode recording from deep brain nuclei. In: Hallett, I.M. (ed.) *Movement Disorder, Handbook of Clinical Neurophysiology*. Elsevier, Amsterdam (2003)
64. Israel, Z., Burchiel, K.: *Microelectrode Recording in Movement Disorder Surgery*. Thieme, Stuttgart (2004)
65. Park, C., Worth, R.M., Rubchinsky, L.L.: Fine temporal structure of beta oscillations synchronization in subthalamic nucleus in Parkinson's disease. *J. Neurophysiol.* **103**(5), 2707–2716 (2010)
66. Hurtado, J.M., Rubchinsky, L.L., Sigvardt, K.A.: Statistical method for detection of phase-locking episodes in neural oscillations. *J. Neurophysiol.* **91**(4), 1883–1898 (2004)

67. Hurtado, J.M., et al.: Temporal evolution of oscillations and synchrony in GPi/muscle pairs in Parkinson's disease. *J. Neurophysiol.* **93**(3), 1569–1584 (2005)
68. Le Van Quyen, M., et al.: Comparison of Hilbert transform and wavelet methods for the analysis of neuronal synchrony. *J. Neurosci. Methods* **111**(2), 83–98 (2001)
69. Ahn, S., Park, C., Rubchinsky, L.L.: Detecting the temporal structure of intermittent phase locking. *Phys. Rev. E* **84**(1), 016201 (2011)
70. Terman, D., et al.: Activity patterns in a model for the subthalamic network of the basal ganglia. *J. Neurosci.* **22**(7), 2963–2976 (2002)
71. Mallet, N., et al.: Parkinsonian beta oscillations in the external globus pallidus and their relationship with subthalamic nucleus activity. *J. Neurosci.* **28**(52), 14245–14258 (2008)
72. Wilson, C.J.: Basal Ganglia. In: Shepherd, G.M. (ed.) *The Synaptic Organization of the Brain*. Oxford University Press, New York (2004)
73. Smith, Y., et al.: Microcircuitry of the direct and indirect pathways of the basal ganglia. *Neuroscience* **86**(2), 353–387 (1998)
74. Bolam, J.P., et al.: Synaptic organisation of the basal ganglia. *J. Anat.* **196**(Pt 4), 527–542 (2000)
75. Buzsaki, G., Traub, R.D., Pedley, T.A.: The cellular basis of EEG activity. In: Ebersole, J.S., Pedley, T.A. (eds.) *Current Practice of Clinical Electroencephalography*, pp. 1–11. Lippincott Williams & Wilkins, Philadelphia (2003)
76. Mitzdorf, U.: Current source-density method and application in cat cerebral cortex: investigation of evoked potentials and EEG phenomena. *Physiol. Rev.* **65**(1), 37–100 (1985)
77. Wilson, C.L., Puntis, M., Lacey, M.G.: Overwhelmingly asynchronous firing of rat subthalamic nucleus neurones in brain slices provides little evidence for intrinsic interconnectivity. *Neuroscience* **123**(1), 187–200 (2004)
78. Stanford, I.M., Cooper, A.J.: Presynaptic mu and delta opioid receptor modulation of GABA IPSCs in the rat globus pallidus in vitro. *J. Neurosci.* **19**(12), 4796–4803 (1999)
79. Ogura, M., Kita, H.: Dynorphin exerts both postsynaptic and presynaptic effects in the Globus pallidus of the rat. *J. Neurophysiol.* **83**(6), 3366–33676 (2000)
80. Cooper, A.J., Stanford, I.M.: Dopamine D2 receptor mediated presynaptic inhibition of striatopallidal GABA(A) IPSCs in vitro. *Neuropharmacology* **41**(1), 62–71 (2001)
81. Shen, K.Z., Johnson, S.W.: Presynaptic dopamine D2 and muscarine M3 receptors inhibit excitatory and inhibitory transmission to rat subthalamic neurones in vitro. *J. Physiol.* **525**(Pt 2), 331–341 (2000)
82. Floran, B., et al.: Dopamine D4 receptors inhibit depolarization-induced [3H]GABA release in the rat subthalamic nucleus. *Eur. J. Pharmacol.* **498**(1–3), 97–102 (2004)
83. Shen, K.Z., et al.: Dopamine receptor supersensitivity in rat subthalamus after 6-hydroxydopamine lesions. *Eur. J. Neurosci.* **18**(11), 2967–2974 (2003)
84. Cragg, S.J., et al.: Synaptic release of dopamine in the subthalamic nucleus. *Eur. J. Neurosci.* **20**(7), 1788–1802 (2004)
85. Shen, K.Z., Johnson, S.W.: Dopamine depletion alters responses to glutamate and GABA in the rat subthalamic nucleus. *NeuroReport* **16**(2), 171–174 (2005)
86. Baufreton, J., Bevan, M.D.: D2-like dopamine receptor-mediated modulation of activity-dependent plasticity at GABAergic synapses in the subthalamic nucleus. *J. Physiol.* **586**(8), 2121–2142 (2008)
87. Park, C., Worth, R., Rubchinsky, L.L.: Neural dynamics in Parkinsonian brain: the boundary between synchronized and nonsynchronized dynamics. *Phys. Rev. E* **83**(4), 042901 (2011)
88. Hernandez, A., et al.: Control of the subthalamic innervation of the rat globus pallidus by D2/3 and D4 dopamine receptors. *J. Neurophysiol.* **96**(6), 2877–2888 (2006)
89. Baufreton, J., et al.: Dopamine receptors set the pattern of activity generated in subthalamic neurons. *FASEB J.* **19**(13), 1771–1777 (2005)
90. Ramanathan, S., et al.: D2-like dopamine receptors modulate SKCa channel function in subthalamic nucleus neurons through inhibition of Cav2.2 channels. *J. Neurophysiol.* **99**(2), 4424–4459 (2008)
91. Park, C., Rubchinsky, L.L.: Intermittent synchronization in a network of bursting neurons. *Chaos* **21**, 033125 (2011)
92. Rabinovich, M., Huerta, R., Laurent, G.: Neuroscience. Transient dynamics for neural processing. *Science* **321**(5885), 48–50 (2008)
93. Tsuda, I.: Hypotheses on the functional roles of chaotic transitory dynamics. *Chaos* **19**(1), 015113 (2009)
94. Hurtado, J.M., Rubchinsky, L.L., Sigvardt, K.A.: The dynamics of tremor networks in Parkinson's disease. In: Bezard, E. (ed.) *Recent Breakthroughs in Basal Ganglia Research*, pp. 249–266. Nova Publishers, New York (2006)
95. Rosenblum, M., Pikovsky, A.: Delayed feedback control of collective synchrony: an approach to suppression of pathological brain rhythms. *Phys. Rev. E, Stat. Nonlinear Soft Matter Phys.* **70**(4 Pt 1), 041904 (2004)
96. Popovych, O.V., Hauptmann, C., Tass, P.A.: Control of neuronal synchrony by nonlinear delayed feedback. *Biol. Cybern.* **95**(1), 69–85 (2006)
97. Tukhlina, N., et al.: Feedback suppression of neural synchrony by vanishing stimulation. *Phys. Rev. E, Stat. Nonlinear Soft Matter Phys.* **75**(1 Pt 1), 011918 (2007)